Lasers in Manufacturing Conference 2021

Spatially resolved melt pool monitoring for process characterization in laser powder bed fusion (LPBF)

Dieter Tyralla[a,*], Peer Woizeschke[a], Thomas Seefeld[a]

[a]*BIAS – Bremer Institut für angewandte Strahltechnik GmbH*

Abstract

Laser powder bed fusion (LPBF) is a frequently used manufacturing process for complex shaped geometries, e.g. bionic structures. The part quality often depends not only on process parameters but also on geometrically induced changes in thermal conditions. Thus, already identified parameters may need to be adjusted to the geometry. Here, a temperature measurement provides information about the current process state due to its recognition of heat input, accumulation and conduction during build-up and thus assists the parameter development.
The present work applies a spatially resolved temperature measurement for process monitoring in LPBF using 2-channel-pyrometry. A lateral resolution of 10 µm is achieved within the complete build-up volume of 250x250x250 mm³ by the coaxial integration of the pyrometric camera system into the beam path of a LPBF machine. The melt pool area was identified as a suitable indicator which enables the prediction of part density during build-up process.

Keywords: Additive manufactruing; Laser powder bed fusion; process monitoring; temperature field measurement; melt pool geometry

1. Introduction

LPBF is a layer wise production technique that enables the manufacturing of metallic parts with complex 3-dimensional geometry. The part density is one of the most important properties in LPBF because of the influences on mechanical properties. Often, the density of the printed parts must be checked by destructive testing or a cost expensive non-destructive CT-measurement to prove their properties.

The part density depends mainly on the process parameters like laser power, welding speed and layer thickness, but it is also influenced by the part geometry which varies for each component. Essentially, a high

* Corresponding author. Tel.: +49-421-218-58114; fax: +49-421-218-58063 .
E-mail address: tyralla@bias.de .

density is achieved for a suitable ratio of the energy introduced and the volume of metal to be melted. A high energy input leads to deep penetration which generates gas pores in the part. Lack of fusion might take place for low energy input. It is commonly known that the temperature field in the process zone indicates the energy balance and can be used to identify applicable parameters.

The most common method for the temperature measurement in LPBF is a lateral camera or a coaxial pyrometer measurement (Islam et al., 2013). Generally, the lateral observation requires a high number of pixels to resolve the tiny melt pools within the large build area (Lough et al., 2020). Otherwise, only a small region in the build area can be observed (Furumoto et al., 2014). In other cases, pyrometers in the near infrared range are integrated coaxially into the beam path (Forien et al., 2020). Here, the observation can be disturbed by spatter and powder that attenuates the process zone (Pavlov et al.; 2010). Thus, 2-channel pyrometers are preferred for the measurement. However, these sensors only provide single-spot temperature values (Gutknecht et al., 2020). The coaxial integration of IR-cameras provides space-resolved temperature field information but is limited however because of the optical properties of common lenses and mirrors in LPBF.

The present work uses a novel 2-channel-pyrometer camera that enables the emissivity corrected temperature field measurement in other applications (Tyralla et al., 2020) and transfers the approach to the LPBF process.

2. Experimental setup

A commercial LPBF machine (Realizer SLM 250) is used for the investigation. The build-up volume is 250 mm by 250 mm by 300 mm. A single-mode fiber laser provides a maximum laser power of 200 W at a wavelength of 1070 nm. The laser spot diameter is measured by 2^{nd}-momentum method and is 50 µm. 20 mm thick steel plates of 1.0570 are used as substrate. A nickel-based alloy (Praxair, TruForm™ HX) is used as powder material with a particle size distribution between 15 µm and 45 µm.

A 2-channel-pyrometer camera (PyroCam, IMS Chips) is used for online temperature field analysis. The camera compares the radiation at 661 nm and 667 nm for an emissivity corrected temperature measurement between 650 °C and 1900 °C. The camera is integrated coaxially into the beam path by the help of a beam splitter like illustrated in fig. 1. The mirrors of the scanner unit are coated for higher reflectivity for laser radiation at 1070 nm and thermal radiation at 650 nm to ensure simultaneous processing and measurement. In addition, a special F-θ lens is used for high transmission in the mentioned spectral ranges, too. The camera manufacturer calibrates the PyroCam for the entire optical path. The accuracy is specified with 2%. This method ensures a process monitoring that follows the laser movement during build up with high frequency and enable the observation of the immediate area around the melting process with high resolution.

A LabView based evaluation algorithm is used for thermal image processing. The melt pool geometry is determined duo to the detection of a bright area in each image that exceeds the melt temperature of the powder material of 1260 °C. The melt pool width, the length and the size are employed as thermal indicators for the process like shown in fig. 1. A detailed description of the setup is given in a previous publication (Tyralla et al., 2021).

Images at different positions in the build-up area are taken to determine the lateral resolution of the camera and to calculate the effect of chromatic aberration. Furthermore, a second thermal calibration is done for the used optical setup by a blackbody radiator for a temperature range between 1200 °C and 1300 °C. The calibration source holds the set temperature to within 1 °C.

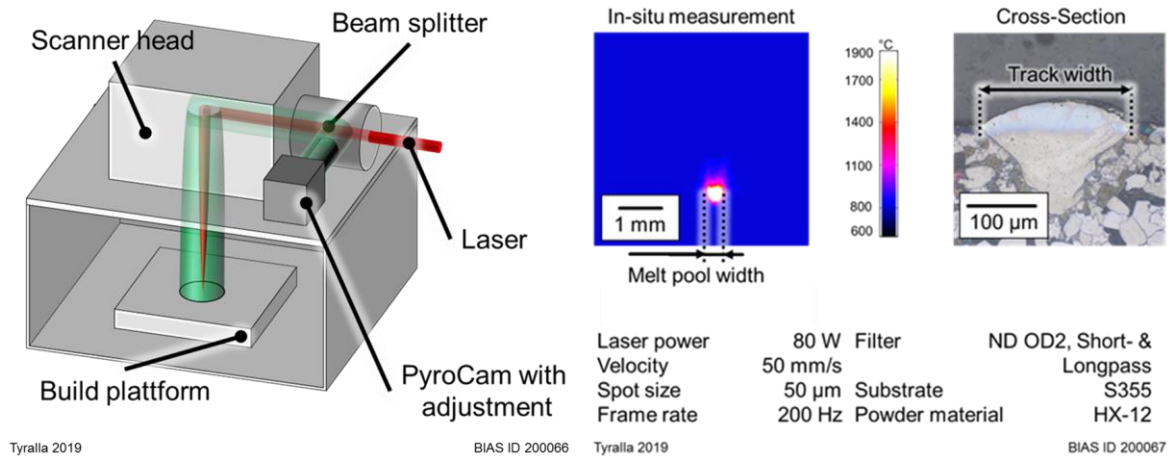

Fig. 1. Schematic of experimental set-up (left) and evaluation of PyroCam images (right). Comparison of PyroCam measured melt pool size and cross-section track width (Tyralla et al., 2021).

Cubes of 10 mm by 10 mm by 10 mm are built up with different parameters. The laser power is adjusted to 80 W, 110 W, 130 W, 170 W and 200 W. The welding speed is varied for all laser powers from 100 mm/s to 500 mm/s. The layer height is 50 µm. The hatches of one layer are made up of patches of 3 mm by 3 mm. At the end of a layer the contour is welded. The welding direction is rotated by 79 ° for the next layer. The tracks are observed by the PyroCam with a framerate of 200 Hz.

3. Results

The lateral resolution of the camera is determined at different positions in the build area. Therefore, the scanner is deflected 50 mm from center position in every direction in the build area. The correlation of lateral dimension in millimeter and pixel of the camera is measured like shown in fig. 2. One pixel size of the PyroCam is 9.1 µm in the entire build area.

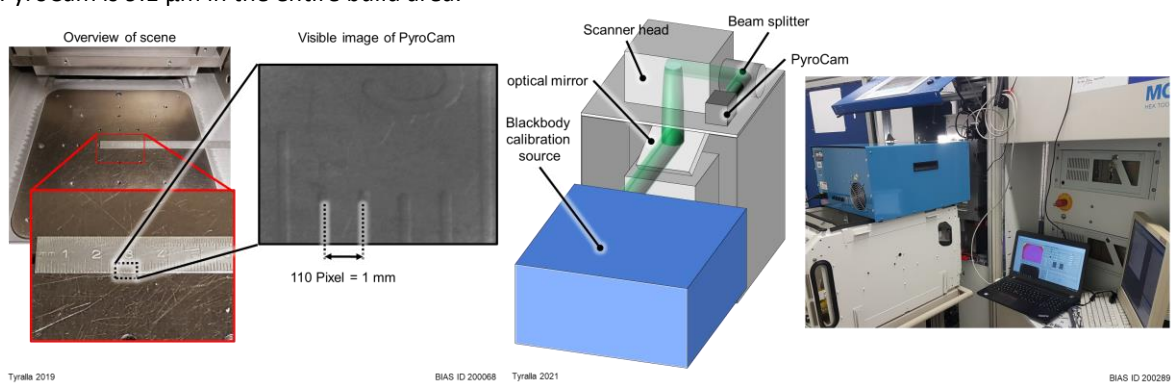

Fig. 2. LPBF chamber with ruler for lateral resolution measurement (left). Picture and schematic of the experimental setup for thermal calibration (right).

The chromatic aberration of the measurement system is calculated by the deviation between laser deflection at 1070 nm and deflection of the optical image of the camera at about 650 nm. Therefore, images of a ruler at maximum scanner deflections are compared. The chromatic aberration in x- and y-direction is 0.013 mm/mm and 0.01 mm/mm, respectively.

The set-up for the thermal calibration is also shown in fig. 2. The thermal radiation of the blackbody is directed by a mirror to the camera. Temperatures between 1200 °C and 1300 °C are measured to prove the specification of the manufacturer for the given melt temperature at 1260 °C. The measured value is compared to the set temperature value of the calibration source. A period of 30 min was used to reach thermal equilibrium for each temperature step. Table 1 show the comparison which indicates for the investigated temperature range always a higher measured value. The averaged relative deviation is 1.7% which is in accordance with the value of the manufacturer.

Table 1. Comparison of camera measured temperature value and set temperature of blackbody calibration source.

Set Temperature [°C]	1200	1250	1300	Avg.
Averaged Temp of PyroCam [°C]	1240	1268	1307	
Standard deviation [K]	19	23	26	
Deviation [%]	3.3	1.4	0.5	1.7

Fig. 3 shows the PyroCam signal of the melt pool area during the build-up process of cubes for the first layer indicated by the black line and the 35th layer indicated by the red line. Here, the entire layer is observed, starting with the first cube with 100 mm/s and 80 W followed by higher laser powers. After the cube that is built with 200 W, the next line of cubes starts with a higher welding speed and 80 W again. After the last cube with 500 mm/s and 200 W, the contour is welded in the same sequence starting with 100 mm/s and 80 W. The average value and the standard deviation for both layers are shown on the right side in fig. 3.

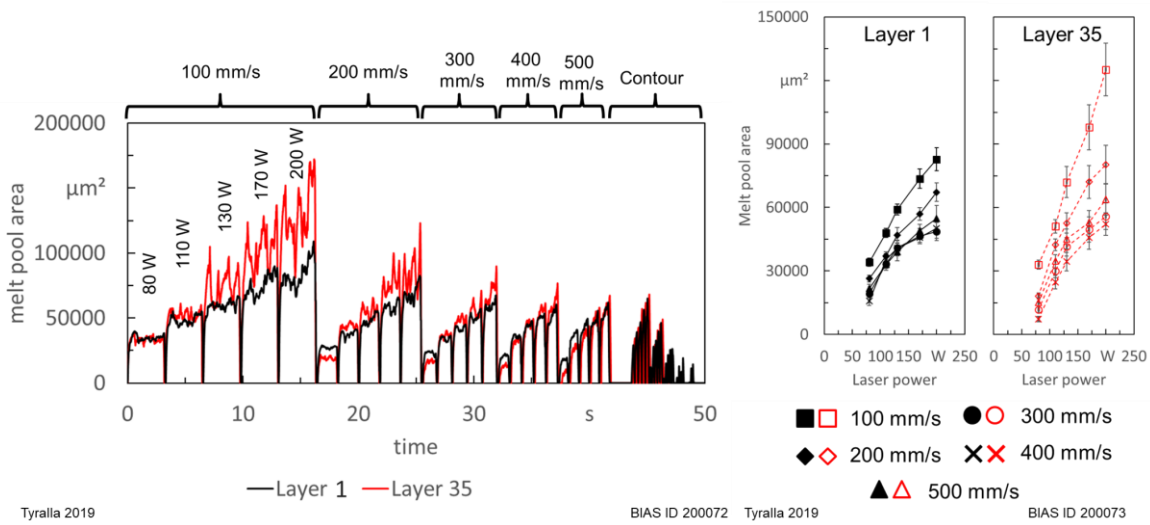

Fig. 3. PyroCam measured melt pool area signal during entire layer 1 and layer 35 (left) and mean value with standard deviation (right) (Tyralla et al., 2021).

The melt pool area increases for higher laser powers and lower welding speeds like already known from the state of the art. In case of the 35th layer, the values rise to a higher level. It is suggested that the heat dissipation is obstructed by the smaller heat conduction of the build material compared to the heat conduction of substrate material. The lower heat flux leads to heat accumulation in the part.

The results of thermal evaluation are correlated to the corresponding values of part density. The values suggest a dependency between melt pool area and part density. A maximum part density can be identified for a melt pool area of 35.000 µm² like shown in fig 4.

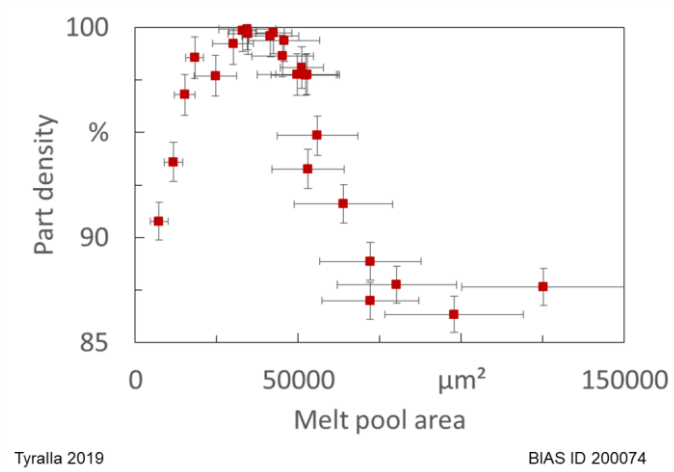

Fig. 4. Correlation of PyroCam measured melt pool area and corresponding part density (Tyralla et al., 2021).

4. Discussion

It is suggested that a smaller melt pool and a larger melt pool increase the porosity by lack of fusion and deep penetration, respectively. Cross-sections of the corresponding samples prove this suggestion by the shape of the pores. Here, smaller melt pools lead to elongated pores that mainly appears between layers and between contour and volume. More round pores are formed for large melt pools which indicating gas inclusions.

It can be noticed that the coefficient of variation significantly increases for melt pool areas larger than the density maximum at 35.000 µm². It is suggested that the higher coefficient of variation results from stronger melt pool dynamics that is caused from deep penetration and melt pool overheating.

The setup shows some systematic errors that are discussed in detail elsewhere (Tyralla et al., 2021). Lateral and thermal deviations are small in the temperature range of interest. It was found, however, that chromatic aberration induces a significant deviation of laser irradiation position and measurement position in the build area. The deviation is approximately 1 mm per 100 mm for the wavelength of the laser and the PyroCam at 1070 nm and around 650 nm, respectively. Thus, the deviation is higher than 10 times the melt pool size. However, the camera-based observation enables the correction of this error and ensures a high resolution and high accuracy for melt pool geometry evaluation during process.

The correlation of part density and melt pool area demonstrates that the lateral resolution is high enough to identify suitable parameters and enable the validation of the parts density already during the process runtime by a measurement of the melt pool geometry.

5. Conclusion

A novel temperature measurement system was integrated on-axis into a commercial LPBF machine. The 2-channel-pyrometer method ensures emissivity corrected temperature field measurement with a frame rate of 200 Hz. The system was characterized regarding lateral and thermal measuring accuracy. The coaxial integration enables a high lateral resolution of less than 0.010 mm in the entire build area of 250 mm by 250 mm. The thermal accuracy was verified by a blackbody and is 1.7% in the temperature range of interest. The chromatic aberration is determined and automatically corrected by the 2-dimensional evaluation method.

It was shown for the first time that the melt pool area is a meaningful indicator for process behavior in build-up process. This value correlates to the part density and enables the validation of different processes during build up. Thus, the basis for a closed loop control system was established that allows a continuous product documentation and has the potential to reduce or avoid a cost and time expensive NDT-analysis.

Acknowledgements

The work was funded by the Bremer Luft- und Raumfahrtfroschungsprogramm 2020 under contract no. LURAFO3001C from funds of the European Union, of the European Regional Development Fund and the state of Bremen, which the authors gratefully acknowledge.

European Union
Investing in Bremen's Future
European Regional
Development Fund

References

Forien, J.-B., Calta, N. P., DePond, P. J., Guss, G. M., Roehling, T. T., Matthews, M. J., 2020. Detecting keyhole pore defects and monitoring process signatures during laser powder bed fusion: A correlation between in situ pyrometry and ex situ X-ray radiography, Additive Manufacturing Vol.35, 101336. DOI: 10.1016/j.addma.2020.101336.

Furumoto, T., Ueda, T., Alkahari, M., Hosokawa, A., 2013. Investigation of laser consolidation process for metal powder by two-color pyrometer and high-speed video camera, CIRP Annals - Manufacturing Technology 62, p.223–226.

Gutknecht, K., Haferkamp, L., Cloots, M., Wegener, K., 2020. Determining process stability of Laser Powder Bed Fusion using pyrometry, Procedia CIRP Vol.95, p. 127-132, DOI: 10.1016/j.procir.2020.01.147.

Islam, M., Purtonen, T., Piili, H., Salminen, A., Nyrhila, O., 2013. Temperature profile and imaging analysis of laser additive manufacturing of stainless steel, Physics Procedia 41, p. 835 – 842

Lough, C.S., Wang, X., Smith, C.C., Landers, R.G., Bristow, D. A., Drallmeier, J.A., Brown, B., Kinzel, E.C., 2020. Correlation of SWIR imaging with LPBF 304L stainless steel part properties, Additive Manufacturing Vol. 35, 101359. DOI: 10.1016/j.addma.2020.101359.

Pavlov, M., Doubenskaia, M., Smurov, I., 2010. Pyrometric analysis of thermal processes in SLM technology, Physics Procedia 5, p. 523–531.

Tyralla, D.; Köhler, H.; Seefeld, T.; Thomy, C.; Narita, R., 2020. A multi-parameter control of track geometry and melt pool size for laser metal deposition. In: Procedia CIRP 94, p. 430-435

Tyralla, D., Seefeld, T., 2021. Thermal Based Process Monitoring for Laser Powder Bed Fusion (LPBF), Advanced Materials Research Vol. 1161, p. 123-130. DOI: 10.4028/www.scientific.net/AMR.1161.123